‘Frustrated’ hydrogen bonded self-associated systems as templates towards DNA incorporated nanostructure formation†

Tamrin L. Gumbs,[a] Lisa J. White,[a] Neil J. Wells,[b] Helena J. Shepherd[a] and Jennifer R. Hiscock*[a]

[a] *Dr J. R. Hiscock, School of Physical Sciences, University of Kent, Canterbury, UK, CT2 7NH; E-mail: J.R.Hiscock@Kent.ac.uk; Tel: +44(0)1227 816467.*

[b] *School of Chemistry, University of Southampton, Southampton, UK, SO17 1BJ.*

This work was supported by the Army Research Office (US) under grant W911NF-16-1-0247 and the University of Kent under the Caldin Fellowship. The authors would like to thank K. Howland for his assistance with mass spectrometry during the project.

† Electronic Supplementary information (ESI): This includes experimental details, NMR and crystallography data. See DOI:

‘Frustrated’ hydrogen bonded self-associated systems as templates towards DNA incorporated nanostructure formation.†

Herein, we present the synthesis of a thymine nucleobase appended ‘frustrated’ monomer, which exhibits self-association in DMSO solutions through the formation of hydrogen bonds. This self-association process has been explored in both competitive DMSO solutions and the solid state, using a combination of NMR and single crystal X-ray diffraction techniques. The self-associative equilibria within the solution state are balanced in such a way that the hydrogen bond donating (HBD) and accepting (HBA) thymine residue present within the monomeric structure is free to coordinate further guest species such as the complimentary DNA base adenine. The adenine simulants, 2-aminopyridine and 2,6-diaminopyridine have been used to explore the potential of these self-associated structures towards the coordination of complimentary DNA base pairs.

Keywords: self-association; hydrogen bonding; host-guest chemistry

† Electronic Supplementary information (ESI): This includes experimental details, NMR and crystallography data. See DOI:

1. Introduction

Molecular self-association and resultant nanostructure formation typically rely on supramolecular interactions such as hydrogen bonding, electrostatics and charge transfer.[1,2] As a consequence, supramolecular principles are now being effectively used within the design of novel self-associated systems, giving rise to controlled aggregation events and stimulating a move towards programmable nanostructure,[2-6] supramolecular organic framework[7] and supramolecular gel design.[8,9] This has included work by Zhao and co-workers[10] who have shown the potential of hydrogen bonded, self-associated amphiphiles towards the development of novel drug/gene nanocarriers; Atwood and co-workers[11] who have shown supramolecular frameworks synthesised from pyrogallol[4] arene and 4,4'-bipyridine-type spacers to be solvent stable; and Steed and co-workers[12] who showed that hydrogen bonded linkages could replace covalent bonds in the design

of supramolecular gelators. Work such as this showcases the importance of hydrogen bond formation in the control self-association events, and therefore the fundamental need to understand how to control these interactions at the molecular level.

Although the formation of hydrogen bonded urea:anion hydrogen bonded complexes is well known,[13,14] the self-associating properties of anion-spacer-urea amphiphilic monomers were first probed in the solution state by Faustino and co-workers.[15] Members from this class of compound were shown to exhibit similar critical micelle concentrations to sodium decanoate;[16] these properties were attributed to intermolecular hydrogen bonding interactions. In our preliminary studies,[17,18] we extended this work using similar amphiphilic monomers with the basic structure shown in Figure 1. These systems are 'frustrated' in the sense that they cannot fulfil all of their potential self-associative hydrogen bonding modes simultaneously as they contain a single hydrogen bond donating (HBD) urea functionality but two hydrogen bond accepting (HBA) sulfonate and urea groups. These compounds can form tapes through both urea-anion and urea-urea complex formation events in the solid state.[17] They may also form dimeric species with the stability of these complexes maintained through intermolecular sulfonate-urea hydrogen bonded complex formation. We were able to show that a preference of any one of these binding modes could be modulated through the alteration of HBD acidity or the strength of counter cation coordination. Moving into the solution state,[18] we were able to go some way to controlling the hydrogen bonding modes present in the self-associated structure through the addition of competitive HBD and HBA species. As we are now beginning to gain an understanding of the hydrogen bonding modes involved within these self-associated species, we wish to utilise the nanostructures formed as templates the controllable synthesis of ever more complex nanostructure and material design.

Here we present the first steps to achieving this, though the synthesis of **1** which was synthesised as the tetrabutylammonium (TBA) salt of the anion. This compound contains the same basic urea-spacer-anion motif as our previous 'frustrated' amphiphiles but we have extended the functionality by appending the nucleobase thymine, responsible for hydrogen bonded duplex formation within the DNA double helix. This increases the number of HBD NH and HBA carbonyl functionalities present in our already 'frustrated' system. In this work we show that the controlled balance of these hydrogen-bonded complexation events could lead to the ever more complex controlled assembly of DNA incorporated nanostructures. In order to investigate these systems more thoroughly we also synthesised receptors **2** and **3**, which contain the HBD thymine and urea functionalities respectively, to better understand the roles of these functionalities within possible coordination events in the absence of the self-associated species.

DNA has now moved beyond its traditional biological function to be seen by many as an intelligent construction material, producing two and three dimensional networks with an ever extending role in electronics, diagnostics, medicine, materials science and synthetic biology.[19] More recently the development of DNA inspired supramolecular chemistry[20] has included the use of DNA micelles as nanoreactors[21] and the synthesis of dynamic DNA nanotubes.[22] The use of nucleobases in the construction of supramolecular assemblies and synthetic polymers is also attracting attention.[23] Examples of this include work by Champness and co-workers, who have used thymine appended porphyrins to give a molecule which is capable of square two dimensional network assembly on a planar graphite surface;[24] and O'Reilly and co-workers who have used a combination of block copolymer self-association and complimentary nucleobase complexation for controllable polymer formation.[25]

2. Materials and Methods

2.1 Synthesis

Compound **1** was synthesised from previously published compound **4**.[18] The nitro group of **4** was reduced with hydrazine and Pd/C 10 % in ethanol to give crude **5**. Thymine-1-acetic acid was then activated with carbonyldiimidazole (CDI) in DMF and crude **5** added. The analytically pure product was isolated through precipitation of a white solid from the reaction mixture with the addition of DCM in a yield of 18 %. Receptor **2** was prepared through the reaction of thymine-1-acetic acid with CDI in chloroform, followed by the addition of 4-nitroanaline. The resultant solid was removed by filtration and washed with methanol to give the product as a white solid in a yield of 38 %. Receptor **3** was obtained by reaction of butyl isocyanate with 4-nitroanaline in pyridine. The resultant solution was diluted with chloroform and washed with dilute HCl and water. The organic phase was then dried over magnesium sulfate and the product obtained as a yellow solid in a yield of 47 % through precipitation from chloroform with hexane.

2.2 Single crystal X-ray diffraction

Single crystal diffraction data were collected using a Rigaku Oxford Diffraction Supernova diffractometer, with Cu Kα radiation to a maximum resolution of 0.84 Å. The crystal was kept at 100(1) K during data collection, using an Oxford Cryosystems 800-series Cryostream. Single crystals of **1** are exceptionally prone to damage when removed from the mother liquor, with complete amorphisation taking place within seconds. After several attempts, a well diffracting crystal was mounted on the diffractometer in the cold stream. While crystal decay is reduced at 100 K, diffraction quality significantly decreased during data collection. The low-angle data were

collected first, followed by high-angle data. Unfortunately the crystal quality was reduced to the extent that little diffraction can be observed beyond 1 Å. Subsequent attempts to recollect better quality high-angle data before crystal degradation unsuccessful; however the unit cell of each crystal was found to be equivalent to that reported here for **1** in all cases.

As a consequence of the general poor quality of the data, interpretation of fine structural detail should be approached with caution but, the network structure of anion and cation can nevertheless be unambiguously identified.

The structure was solved with the ShelXT[26] structure solution program using Direct Methods and refined with ShelXL[27] by Least Squares minimisation. Olex2[28] was used as an interface to all ShelX programs. The unit cell contains two monomers of **1,** five molecules of DCM and further disordered solvent that could not be modelled with discrete atomic positions. The *PLATON* SQUEEZE[29] tool was used to remove the contribution of disordered solvent to the calculated structure factors. More details are provided in the cif. All non-hydrogen atoms were refined using anisotropic displacement parameters, and hydrogen atoms were placed at calculated positions. A significant number of restraints and constrains were used to ensure a convergent refinement, also detailed in the cif.

3. Results and Discussion

3.1 Solution state self-association

As DNA complexation typically occurs under highly competitive aqueous conditions our complexation studies were conducted in DMSO or DMSO-water mixtures. At the present time we have not moved into aqueous conditions due to the inherent difficulties

in the observation of NH resonances *via* ^{1}H NMR as a result of deuterium exchange effects. The presence of hydrogen-bond mediated self-association was determined by a ^{1}H NMR dilution study in DMSO-d_6. As illustrated in Figure 2, dilution of the original sample resulted in the upfield perturbation of those signals corresponding to the urea NHs only with increasing concentration of **1**. No change in chemical shift for those resonances corresponding the amide or thymine NHs could be detected, demonstrating that out of the four possible HBD NH groups only the urea functionality is involved in the hydrogen-bonded self-association process under these conditions. Further analysis of the ^{1}H NMR resonances corresponding to the methylene group also showed no change in chemical shift during the course of the dilution experiment, this is further evidence that the thymine functionality is not involved in the self-association process.

The dilution data obtained from the change in chemical shift of the urea NH was fitted to both the dimerization/equal K model (EK)[30,31] where the association constants for all self-associative effects are equal, and the cooperative equal K model (coEK), where the first association constant in the self-association process is different to the subsequent association constants which are all equal, using BindFit v0.5.[32,33] These models assume one component, one dimensional homogeneous aggregation.[34] The association constants calculated for the strength of self-associated complex formation were shown to be < 10 M^{-1} in both cases implying that the self-associative interaction is weak. A better fit was obtained with the equal EK model than the coEK model, which gives evidence for the former being the self-associative mode that exists within the solution state. A ^{1}H ROESY NMR study (Figure 3) also showed through space interactions between the aryl urea NHs and the CH_2 adjacent to the sulfonate functionality, revealing that these two chemical groups are in close proximity within the DMSO-d_6 solution.

An estimation for the size of the self-associated nanostructures of **1** present in a DMSO-d_6 solution, visible by ^{1}H NMR was obtained through DOSY experiments.[35] As shown in Figure 4, the cationic and anionic component of **1** have different diffusion constants, showing that these two species are not strongly coordinated. The ^{1}H NMR DOSY experiments were performed with two different concentrations of **1** (55.6 mM and 5.6 mM). The translational diffusion coefficients (D) obtained from ^{1}H NMR DOSY experiments were then used to calculate hydrodynamic radius (r_H) of the self-associated species in solution, through rearrangement of the Stokes–Einstein equation:

$$D = \frac{k_B T}{6\pi\eta r_H} \qquad (1)$$

where k_B is the Boltzmann constant, T is the temperature and η is the viscosity of the solvent. However, this approximation of the hydrodynamic radius must be treated with caution as it assumes that the diffusing entity is a sphere and that the van der Waals volume of the molecular complex is large compared to that of the solvent.[36] This system also exists in fast exchange, which can cause further complications with data interpretation. [37,38] The TBA counter cation was shown to have a hydrodynamic radius of 0.59 nm and 0.55 nm and the self-associated anionic component was shown to have a hydrodynamic radius of 0.90 nm and 0.81 nm respectively at 55.56 mM and 5.56 mM concentrations.

3.2 Solid state self-association

The single crystal X-ray structure shown in Figure 5 of **1** was obtained by the slow evaporation of DCM into a DMF solution of the salt. As described in the materials and methods section, the crystals obtained were found to be unstable over time which resulted in a decrease in the quality of the data collection. The molecular self-association of **1** can be determined although the data collected do not allow us to calculate hydrogen bond lengths or angles with certainty. The unit cell contains two

crystallographically distinct monomers of **1**, five molecules of DCM and further solvent molecules that could not be resolved. Each of the anionic components of **1** was found to dimerize with a symmetry equivalent to itself (forming two crystallographically distinct dimers) through the formation of four intermolecular sulfonate-urea hydrogen bonds. The dimeric units were calculated to be approximately 1.9 nm by 1.5 nm by 0.8 nm in size. These values are in approximate agreement with those calculated by DOSY NMR which have a hydrodynamic diameter of 1.6 nm (5.56 mM) -1.8 nm (55.56 mM).

Unlike in solution, within the solid state there is limited competition from HBD/HBA solvent molecules, and as a consequence, weaker hydrogen bonds that may be out competed in solution can be observed in the solid state. Further analysis of the extended hydrogen bonded network showed that these dimeric units were able to further self-associate, through the formation of urea oxygen:thymine NH hydrogen bonds, to produce the helical tetrameric units shown in Figure 6.

The tetrameric units formed by each of the two different anionic substituents contained within the unit cell are able to further independently self-associate through the formation of thymine NH:amide O hydrogen bonds to form an extended pseudo porous crystalline structure. These pseudo pores are approximately 27 Å in diameter and contain both the TBA and residual solvent molecules. An extended pseudo porous network is produced by each of the two anionic components within the unit cell. These networks interlink perpendicular to one another to produce a three-dimensional chainmail motif, illustrated in Figure 7.

3.3 Extended host-guest complexation within the solution state

The combination of evidence obtained from ^{1}H NMR DOSY, ^{1}H NMR ROESY, ^{1}H NMR dilution study and X-ray crystal structure determination supports the self-association process of compound **1** in DMSO favouring the formation of urea-anion

rather than urea-urea interactions, as shown in Scheme 1. We further propose that the self-associated solution state structure predominantly includes only a small number of molecular anionic units. We can also assume that the HBD/HBA thymine residue is free to coordinate further guest species. For this reason the images presented within the Scheme 1 have been limited to the self-assembly of two anionic units only.

In order to further probe these self-associated systems towards the eventual coordination of a complimentary base-paired single strand of DNA, as illustrated in Figure 8, 2-aminopyridine (compound **6**) and 2,6-diamino pyridine (compound **7**) were used as adenine simulants. These two simulants have a similar arrangement of HBD and HBA functionalities to that of adenine, the complimentary base pair of thymine. A series of ^{1}H NMR titration studies with **1** vs. these adenine simulants was conducted in a DMSO-d_6 0.5 % water solution. Figures 9a and 9b show the results of these titration studies and the association constants calculated for 1:1 complex formation are given in Table 1. There was no significant change in chemical shift observed with either the aryl urea or amide NH resonances upon the addition of **6** to **1**, showing no evidence of host-guest hydrogen bonded complex formation. The position of the alkyl urea NH resonance was obscured by overlapping signals within the ^{1}H NMR spectra and so could not be observed. However, a downfield change in chemical shift for the resonance corresponding to the thymine NH was observed, indicating the presence of a thymine NH:**6** hydrogen bonded complex. An analogous ^{1}H titration experiment, with **7** again showed no discernible hydrogen-bonded complex formation with either the amide or aryl urea NH groups, but there was a significant change downfield in chemical shift noted for the alkyl urea NH, which in this case was not obscured by any other resonances. Again the most significant downfield change in chemical shift was noted with for the thymine NH. The association constants calculated for each of these 1:1

complexation events were < 10 M^{-1}, demonstrating weak binding. This is unsurprising when considering that in this instance, formation of a neutral molecule complex is observed, theoretically stabilised through as few as two hydrogen bonds in a highly competitive solvent mixture. Nevertheless, this does give an indication as to the type of hydrogen bond complexation that may occur within any DNA incorporated nanostructure.

Due to the complex molecular structure and resultant self-association processes of **1** which may influence any observed host-guest complexation events, receptors **2** and **3** were produced which contain either the thymine and amide or urea HBD moieties respectively but do not experience the self-association effects of **1** as the sulfonate functionality is not present in either receptor structure. As a consequence, the individual complexation events of **1** can be observed independently of the parent system. A series of ^{1}H NMR titrations with both receptors **2** and **3** were conducted in a DMSO-d_6 0.5 % water solution with both adenine simulants and HSO_4^-. The results of these titration studies are shown in Figures 10a and 10b for **2** and **3** respectively. HSO_4^- was used in this instance to establish whether the spatial orientation of the HBD groups in relation to the sulfonate moiety of **1** was responsible for the hydrogen bonding mode present or if it was more strongly influenced simply by preferential complex formation. The association constants calculated from this series of titrations with **2** and **3** are given in Table 1. Interestingly the thymine NH of **2** shows no interaction with HSO_4^-, but there is evidence for hydrogen bond formation with the amide NH. Under these conditions weak hydrogen bonded complexes were observed to form with both the DNA simulants and thymine NH. These DNA simulants were also shown to interact at the amide NH. The analogous set of experiments conducted with **3** showed no significant change in chemical shift upon the addition of **7** however, association constants were calculated for

the hydrogen bonded complexes formed upon the addition of both **6** (43 M^{-1}) and HSO_4^- (27 M^{-1}).

The weak 1:1 hydrogen bonded complexes observed for **2** (amide NH): **7** (28 M^{-1}), **2** (amide NH):HSO_4^- (25 M^{-1}) and **3** (urea NH): **6** (43 M^{-1}) were not observed to form with **1**, indicating that the self-association process affects the type and presence of these hydrogen bonded complexation events. The absence of a **2** (thymine NH):HSO_4^- and the presence of a **3** (urea NH):HSO_4^- bonded complex supports the formation of the urea-anion complex within the self-association of **1** in the solution state.

4. Conclusions

We have synthesised a thymine inspired monomer, based on our previous 'frustrated' amphiphile design which contains a combination of different HBD (urea, thymine and amide) and HBA (carbonyl oxygen and sulfonate) groups. Proton NMR dilution studies suggest that the anionic monomer self-associates through the use of HBD urea groups in a DMSO solution. DOSY NMR experiments indicate that the self-associated structures have a concentration dependent hydrodynamic radius between 0.55-0.59 nm, meaning that only a few anionic units are involved in the formation of the predominant self-associated structure. Although there are several different types of hydrogen bonded self-association possible for **1**, single crystal X-ray structure determination shows the formation of a sulfonate-urea dimer. Single crystal X-ray diffraction analysis also showed that hydrogen bonded network of the anionic component extended into a three dimensional interlinking pseudo porous network.

The formation of the dimeric urea-anion hydrogen bonded complex within solution state is also supported by the results of ^{1}H NMR ROESY and a series of ^{1}H NMR titration experiments. The ^{1}H NMR titration experiments with the adenine

simulant, **6**, showing hydrogen bonded complex formation with the thymine but not the urea or amide NH groups, provides evidence that this type of self-associated structure may be used to produce a novel class of DNA templated nanostructures. Receptors **2** and **3** have allowed the identification of contributions of the different HBD groups separately and independently of the self-associative process experienced by **1**. These studies have confirmed the preferential interaction of HSO_4^- towards the urea and amide NH functionalities over the thymine group. Complexation of the DNA simulants to all HBD functionalities of **2** and **3** suggest that any reversal of this trend with **1** is due to preferential self-associative complexation events.

5. Acknowledgements

This work was supported by the Army Research Office (US) under grant W911NF-16-1-0247 and the University of Kent under the Caldin Fellowship. The authors would like to thank K. Howland for his assistance with mass spectrometry during the project.

6. References

(1) Wang, C.; Wang, Z.; Zhang, X. *Acc. Chem. Res.* **2012**, *45*, 608-618.

(2) Yu, G.; Jie, K.; Huang, F. *Chem. Rev.* **2015**, *115*, 7240-7303.

(3) Kumar, S.; Ludwig, K.; Schade, B.; von Berlepsch, H.; Papp, I.; Tyagi, R.; Gulia, M.; Haag, R.; Boettcher, C. *Chem. Eur. J.* **2016**, *22*, 5629-5636.

(4) Thota, B. N. S.; Urner, L. H.; Haag, R. *Chem. Rev.* **2016**, *116*, 2079-2102.

(5) Wang, J.; Wang, X.; Yang, F.; Shen, H.; You, Y.; Wu, D. *Langmuir* **2015**, *31*, 13834-13841.

(6) Yu, G.; Jie, K.; Huang, F. *Chem. Rev.* **2015**, *115*, 8944-8944.

(7) Tian, J.; Chen, L.; Zhang, D. W.; Liu, Y.; Li, Z. T. *Chem. Commun.* **2016**, *52*, 6351-6362.

(8) Sangeetha, N. M.; Maitra, U. *Chem. Soc. Rev.* **2005**, *34*, 821-836.

(9) Steed, J. W. *Chem. Commun.* **2011**, *47*, 1379-1383.

(10) Zhou, X.; Liu, G.; Yamato, K.; Shen, Y.; Cheng, R.; Wei, X.; Bai, W.; Gao, Y.; Li, H.; Liu, Y.; Liu, F.; Czajkowsky, D. M.; Wang, J.; Dabney, M. J.; Cai, Z.; Hu, J.; Bright, F. V.; He, L.; Zeng, X. C.; Shao, Z.; Gong, B. *Nat. Commun.* **2012**, *3*, 949.

(11) Patil, R. S.; Kumari, H.; Barnes, C. L.; Atwood, J. L. *Chem. Commun.* **2015**, *51*, 2304-2307.

(12) Hooper, A. E.; Kennedy, S. R.; Jones, C. D.; Steed, J. W. *Chem. Commun.* **2016**, *52*, 198-201.

(13) Busschaert, N.; Caltagirone, C.; Van Rossom, W.; Gale, P. A. *Chemical Reviews* **2015**, *115*, 8038-8155.

(14) Gale, P. A.; Caltagirone, C. *Chemical Society Reviews* **2015**, *44*, 4212-4227.

(15) Faustino, C. M. C.; Calado, A. R. T.; Garcia-Rio, L. *Biomacromolecules* **2009**, *10*, 2508-2514; Faustino, C. M. C.; Calado, A. R. T.; Garcia-Rio, L. *J. Phys. Chem. B* **2009**, *113*, 977-982; Faustino, C. M. C.; Calado, A. R. T.; Garcia-Rio, L. *J. Colloid Interface Sci.* **2011**, *359*, 493-498; Faustino, C. M. C.; Calado, A. R. T.; Garcia-Rio, L. *J. Colloid Interface Sci.* **2012**, *367*, 286-292.

(16) Faustino, C. M. C.; Calado, A. R. T.; Garcia-Rio, L. *J. Colloid Interface Sci.* **2010**, *351*, 472-477.

(17) Blackholly, L. R.; Shepherd, H. J.; Hiscock, J. R. *CrystEngComm* **2016**, *18*, 7021-7028.

(18) Hiscock, J. R.; Bustone, G. P.; Wilson, B.; Belsey, K. E.; Blackholly, L. R. *Soft Matter* **2016**, *12*, 4221-4228.

(19) Stulz, E.; Clever, G.; Shionoya, M.; Mao, C. D. *Chem. Soc. Rev.* **2011**, *40*, 5633-5635.

(20) McLaughlin, C. K.; Hamblin, G. D.; Sleiman, H. F. *Chem. Soc. Rev.* **2011**, *40*, 5647-5656.

(21) Trinh, T.; Chidchob, P.; Bazzi, H. S.; Sleiman, H. F. *Chem. Commun.* **2016**, *52*, 10914-10917.

(22) Rahbani, J. F.; Hariri, A. A.; Cosa, G.; Sleiman, H. F. *Acs Nano* **2015**, *9*, 11898-11908.

(23) Surin, M. *Polym. Chem.* **2016**, *7*, 4137-4150.

(24) Slater, A. G.; Hu, Y.; Yang, L.; Argent, S. P.; Lewis, W.; Blunt, M. O.; Champness, N. R. *Chem. Sci.* **2015**, *6*, 1562-1569.

(25) McHale, R.; Patterson, J. P.; Zetterlund, P. B.; O'Reilly, R. K. *Nat. Chem.* **2012**, *4*, 491.

(26) Sheldrick, G. M. *Acta Cryst.* **2015**, *A71*, 3-8.

(27) Sheldrick, G. M. *Acta Cryst.* **2015**, *C71*, 3-8.

(28) Dolomanov, O. V.; Bourhis, L. J.; Gildea, R. J.; Howard, J. A. K.; Puschmann, H. *J. Appl. Cryst.* **2009**, *42*, 339-341.

(29) Spek, A. L. *Acta Crystallogr. C* **2015**, *71*, 9-18.

(30) Evstigneev, M. P.; Buchelnikov, A. S.; Kostjukov, V. V.; Pashkova, I. S.; Evstigneev, V. P. *Supramol. Chem.* **2013**, *25*, 199-203.

(31) Stoesser, P. R.; Gill, S. J. *J. Phys. Chem.* **1967**, *71*, 564-567.

(32) Thordarson, P.; Sewell, K.; Efremova, V. http://supramolecular.org/.

(33) Martin, R. B. *Chem. Rev.* **1996**, *96*, 3043-3064.

(34) von Krbek, L. K. S.; Schalley, C. A.; Thordarson, P. *Chem. Soc. Rev.* **2017**, *46*, 2622-2637.

(35) Patterson, J. P.; Robin, M. P.; Chassenieux, C.; Colombani, O.; O'Reilly, R. K. *Chem. Soc. Rev.* **2014**, *43*, 2412-2425.

(36) Macchioni, A.; Ciancaleoni, G.; Zuccaccia, C.; Zuccaccia, D. *Chem. Soc. Rev.* **2008**, *37*, 479-489.

(37) Chen, A. D.; Johnson, C. S.; Lin, M.; Shapiro, M. J. *J. Am. Chem. Soc.* **1998**, *120*, 9094-9095.

(38) Aguilar, J. A.; Adams, R. W.; Nilsson, M.; Morris, G. A. *J. Magn. Reson.* **2014**, *238*, 16-19.

7. Appendices

Table 1. Association constants calculated (M^{-1}) for **1-3** with DNA simulants (**6** and **7**), and HSO_4^- (supplied as the TBA salt) in a DMSO-d_6 0.5 % water solution at 298 K. These constants were obtained from fitting of ^1H NMR titration data and refined to 1:1 host:guest models using Bindfit.[32]

Guest	**1**			**2**		**3**
	Thymine NH	Amide NH	Urea NH	Thymine NH	Amide NH	Urea NH
6	< 1	a	a	5	a	43
7	< 1	a	4	1	28	a
HSO_4^-	NA	NA	NH	a	25	27

a - Failed to fit/change in chemical shift < 0.1 ppm.

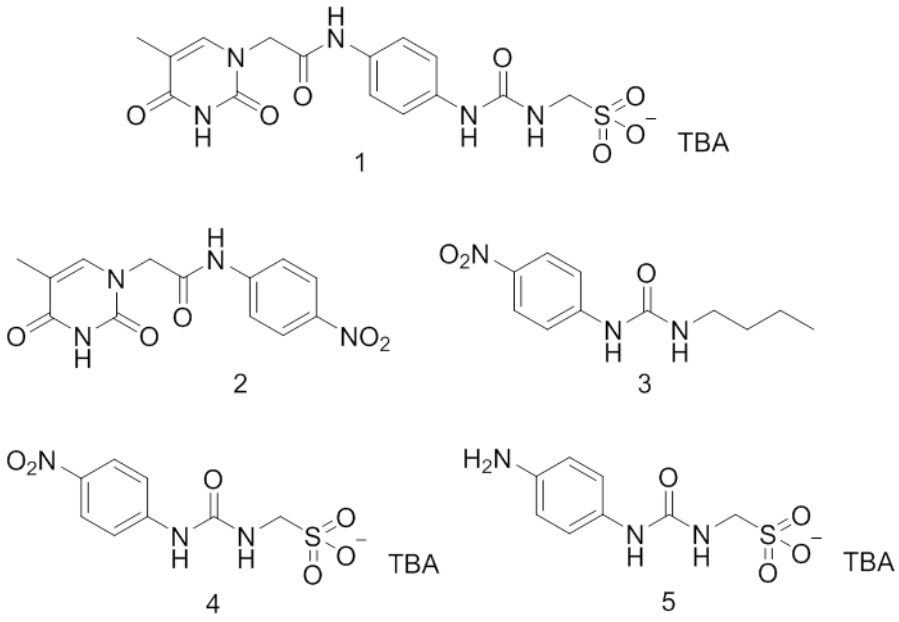

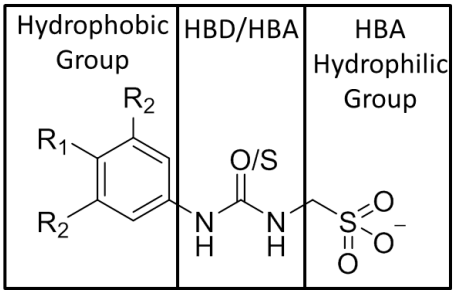

Figure 1. General structure for the anionic component of the sulfonate-urea amphiphilic salts.

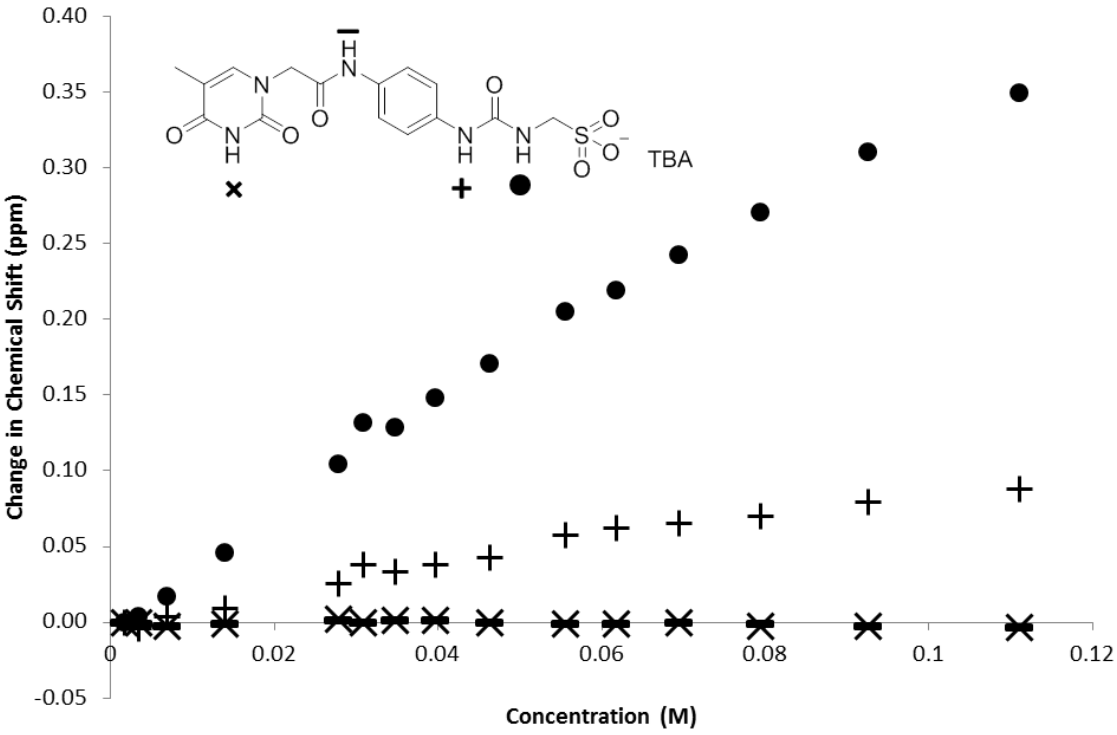

Figure 2. Graph illustrating the ^{1}H NMR downfield change in chemical shift of the NH resonances with increasing concentration of **1** in DMSO-d_6 (298 K).

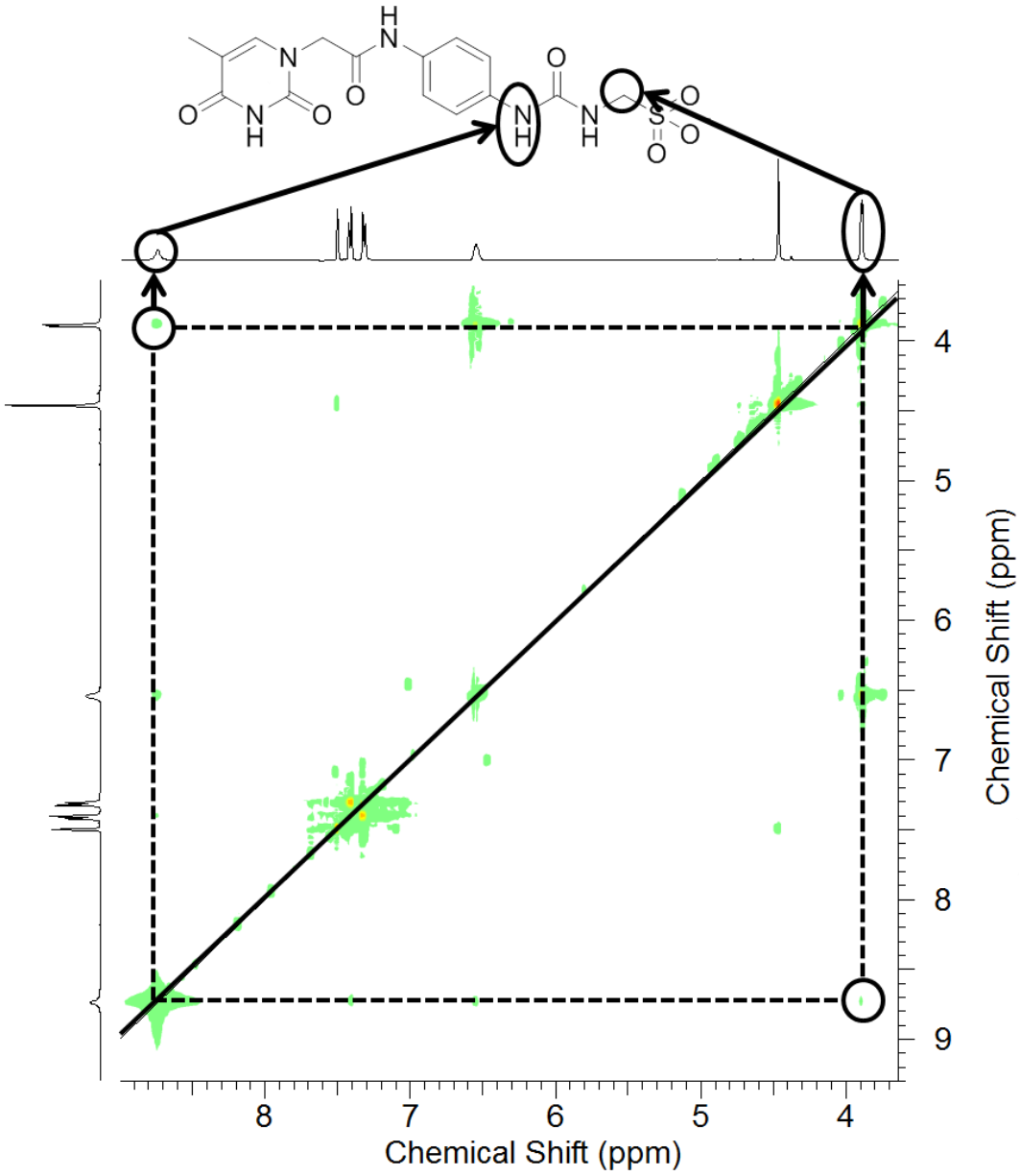

Figure 3. ^{1}H ROESY of **1** (55.6 mM) in DMSO-d_6.

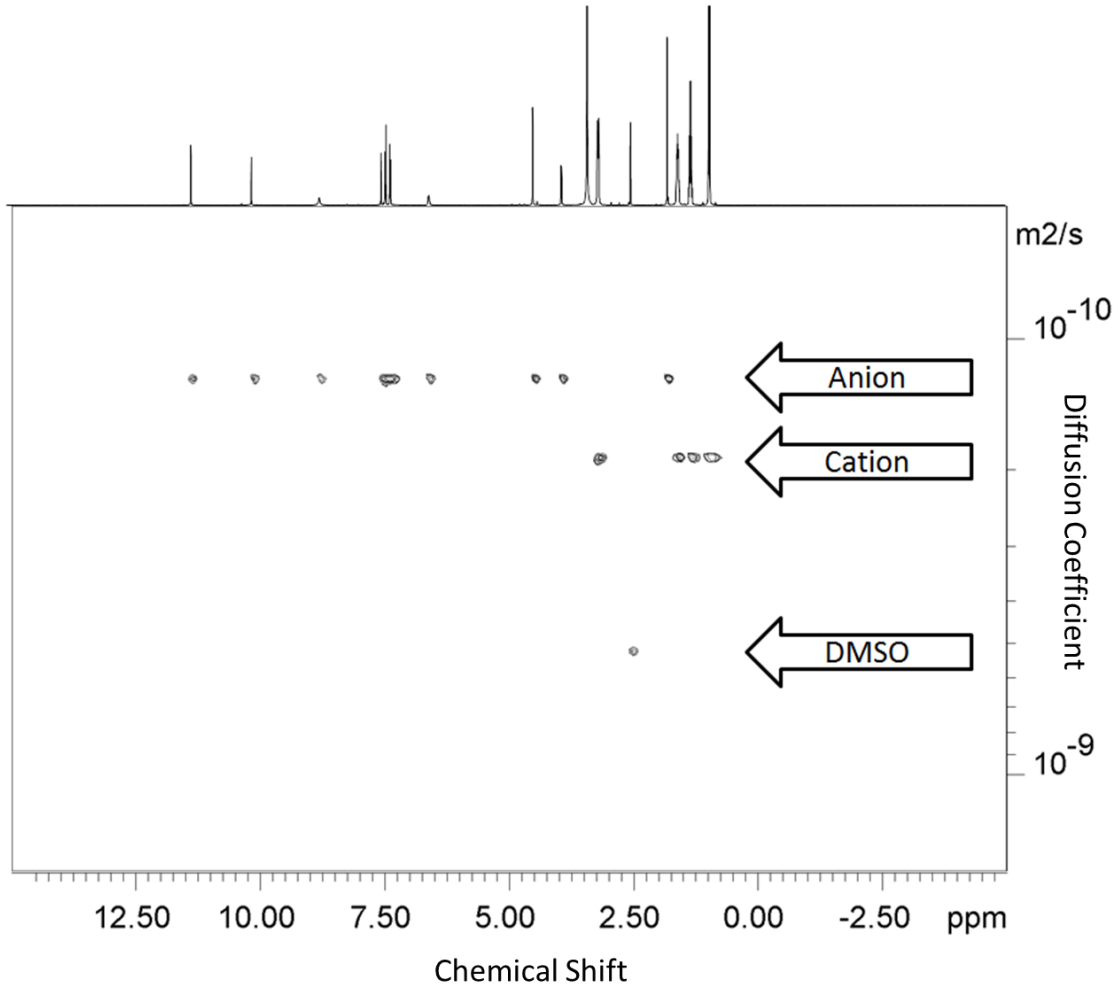

Figure 4. ^{1}H DOSY of **1** (55.56 mM) in DMSO-d_6 conducted at 299.3 K.

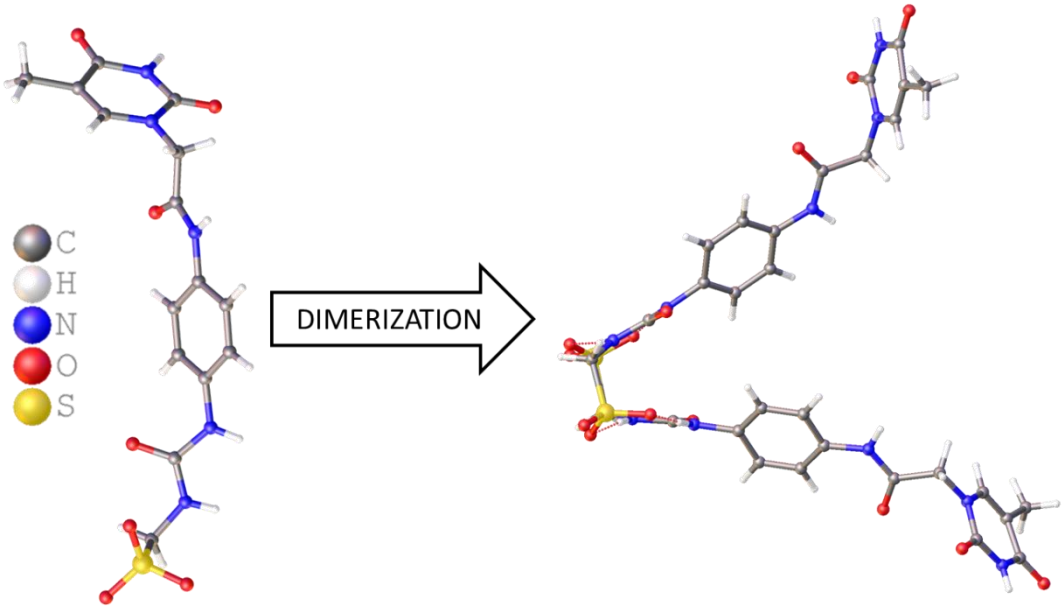

Figure 5. Single crystal X-ray structure of **1**, illustrating dimerization through urea-anion complexation. Residual solvent molecules, second anionic monomer and TBA counter cations have been omitted for clarity.

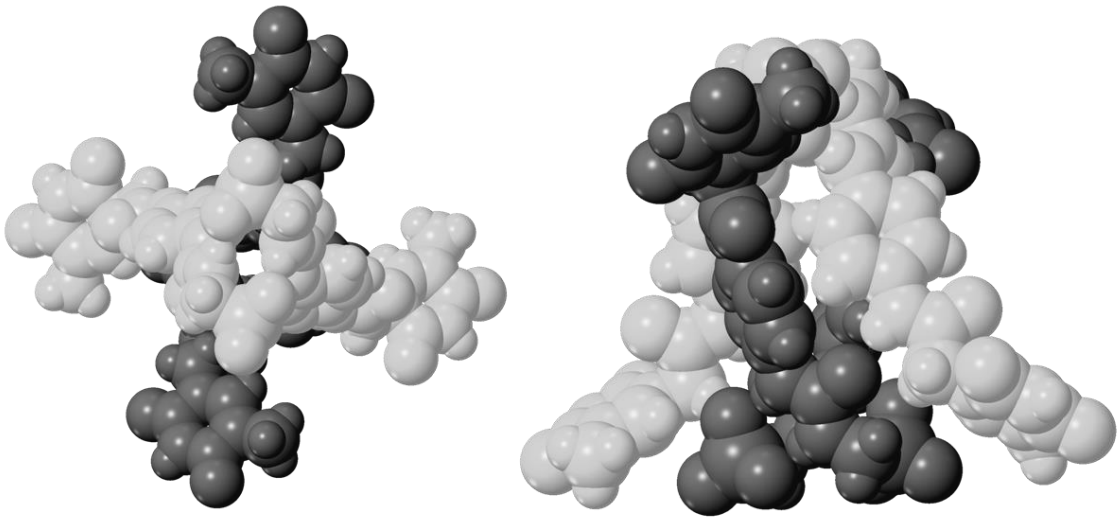

Figure 6. Extended single crystal X-ray structure of a single anionic monomer of **1**, showing tetramer formation through amide NH-urea O hydrogen bond formation between hydrogen bonded dimeric units.

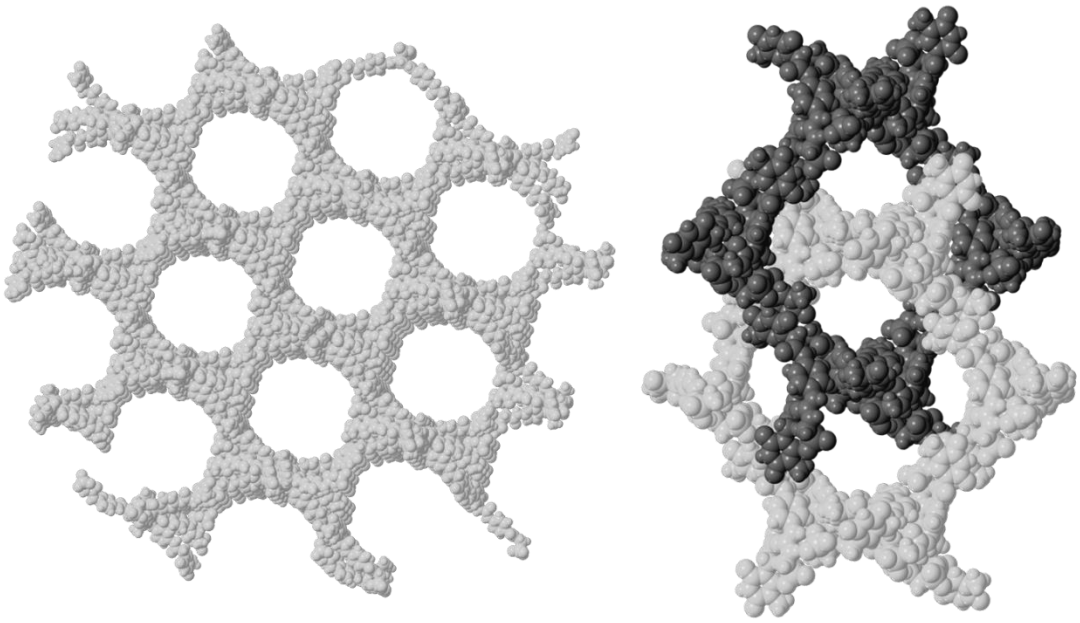

Figure 7. Left) Extended single crystal X-ray structure of a single anionic monomer of **1**, showing a pseudo porous molecular extended strucure through thymine NH-sulfonate hydrogen bond formation between hydrogen bonded tetrameric units. Right) Extended single crystal X-ray structure of both anionic monomers showing interlinking ring systems.

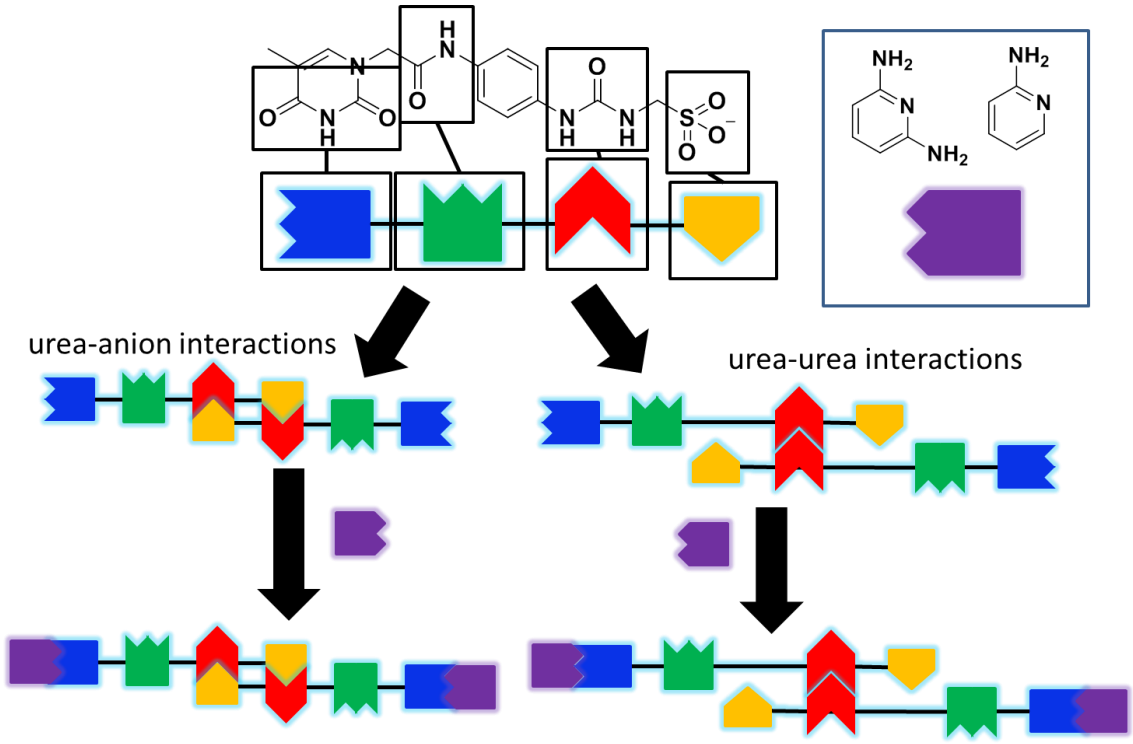

Scheme 1. Possible self-associative and guest coordination hydrogen-bonding modes for **1**.

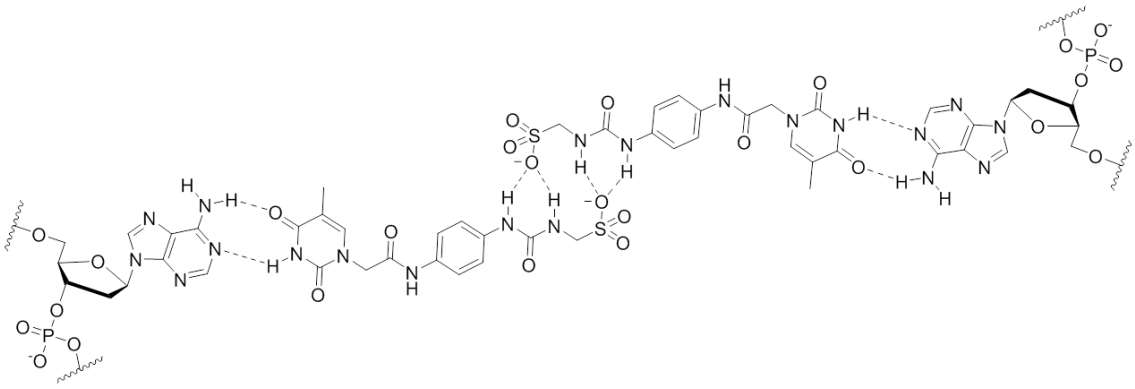

Figure 8. Potential hydrogen bonded coordination of the self-associated structures of **1** with a complimentary single stranded DNA.

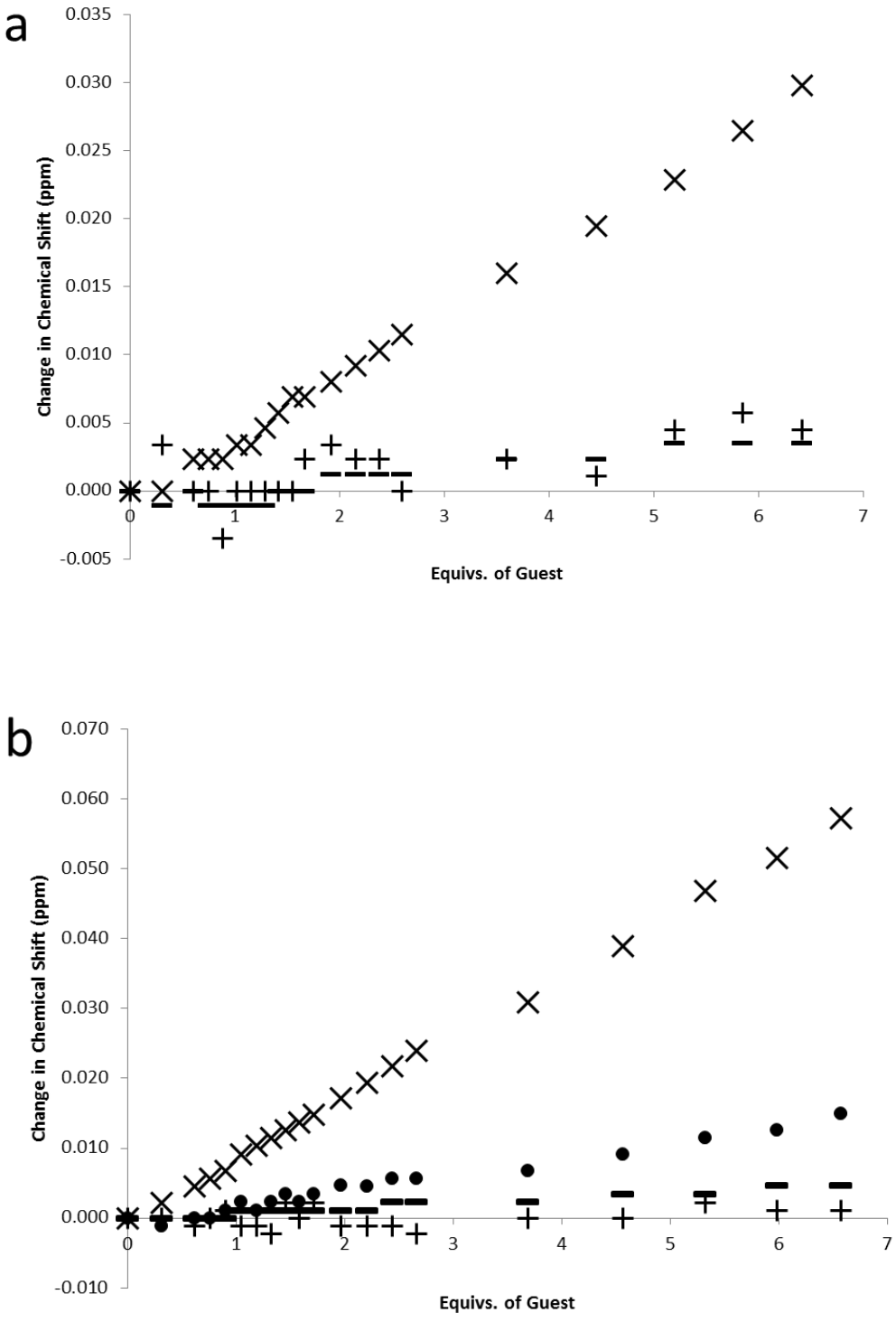

Figure 9. Graph illustrating the downfield change in chemical shift for those signals corresponding to the NH resonances of the thymine (X), alkyl urea (•), aryl urea (+) and amide (-) hydrogen bond donating residues, during a ^{1}H NMR titration of **1** at 298 K with the addition of a) **6** and b) **7**.

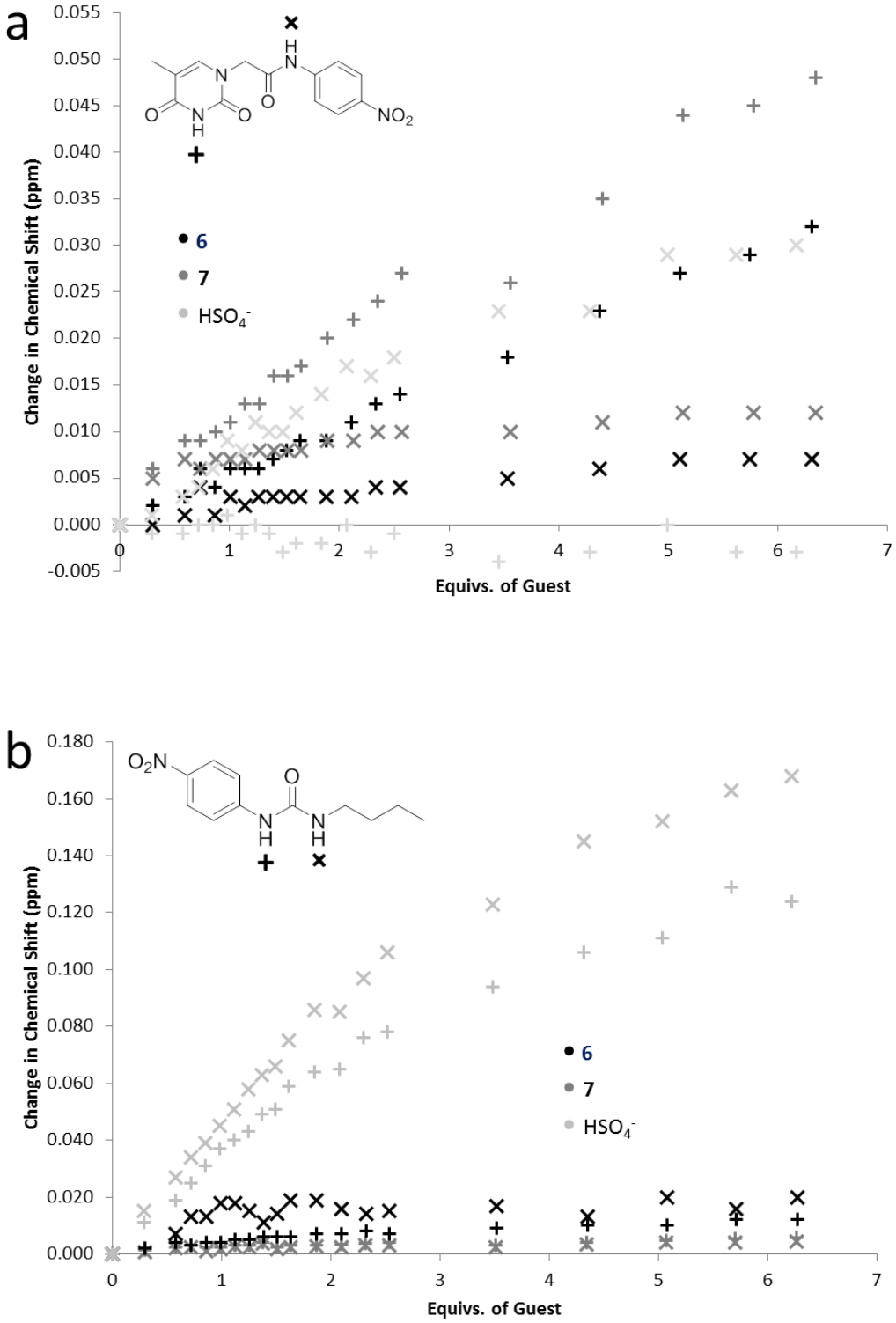

Figure 10. Graph illustrating the downfield change in chemical shift for those signals corresponding to the NH resonances of the hydrogen bond donating residues of a) **2** and b) **3** in the presence of various guest species.